

Reduced Field-of-View Excitation Using Second-Order Gradients and Spatial-Spectral Radiofrequency Pulses

Chao Ma,^{1,2*} Dan Xu,³ Kevin F. King,³ and Zhi-Pei Liang^{1,2}

The performance of multidimensional spatially selective radiofrequency (RF) pulses is often limited by their long duration. In this article, high-order, nonlinear gradients are exploited to reduce multidimensional RF pulse length. Specifically, by leveraging the multidimensional spatial dependence of second-order gradients, a two-dimensional spatial-spectral RF pulse is designed to achieve three-dimensional spatial selectivity, i.e., to excite a circular region-of-interest in a thin slice for reduced field-of-view imaging. Compared to conventional methods that use three-dimensional RF pulses and linear gradients, the proposed method requires only two-dimensional RF pulses, and thus can significantly shorten the RF pulses and/or improve excitation accuracy. The proposed method has been validated through Bloch equation simulations and phantom experiments on a commercial 3.0T MRI scanner. **Magn Reson Med** 69:503–508, 2013.

© 2012 Wiley Periodicals, Inc.

Key words: Radiofrequency pulse design; spatial-spectral radiofrequency pulse; reduced field-of-view excitation; second-order gradient; multidimensional radiofrequency pulse

INTRODUCTION

Multidimensional spatially selective radiofrequency (RF) pulses have wide applications in MR imaging and spectroscopy, which include B_1^+ inhomogeneity correction (1, 2), recovery of susceptibility-induced signal loss (3,4), localized MR spectroscopy (5), and reduced field-of-view (FOV) imaging (6–8). A key limitation of multidimensional RF pulses is their long duration needed to traverse the multidimensional excitation k-space. Recently, parallel excitation techniques have been proposed to shorten multidimensional RF pulses (9,10), although parallel excitation hardware is not yet widely available on commercial MRI scanners.

High-order, nonlinear gradients are another powerful tool that can be exploited to shorten multidimensional RF pulses. Cho and workers first proposed to use pulsed second-order gradients and frequency-selective RF pulses for localized volume excitation (11–13). This method

requires only two one-dimensional RF pulses to excite a circular region-of-interest (ROI) in a thin slice for reduced FOV imaging. However, this method is limited to spin-echo sequences and difficult to be extended to multislice imaging. More recently, PexLoc (parallel excitation using localized gradients) has been proposed to use time-varying high-order gradients for multidimensional RF pulse design (14,15). In PexLoc, conventional multidimensional RF pulse design methods are extended to the case of nonlinear, nonbijective spatial encoding fields, and parallel excitation is used to resolve the inherent encoding ambiguities of such encoding fields. Potential advantages include locally increased spatial resolution (14,16), faster switching time of high-order gradients, and thus shorter RF pulses (15). However, the PexLoc method requires strong and fast-switching high-order gradient fields, which are not available on commercial MRI scanners (17,18).

In this work, we propose a new method to leverage the multidimensional spatial dependence of second-order gradients to design multidimensional RF pulses for reduced FOV imaging. In the proposed method, a spatial-spectral pulse provides a spatial selectivity in the slice direction as well as a spectral selectivity that is transferred into a spatial selectivity by the spatial dependence of the resonance frequency introduced by the second-order gradients. As a result, 3D spatial selectivity (a circular ROI in a thin slice) is achieved by a 2D spatial-spectral RF pulse in the presence of second-order gradients, which can significantly shorten RF pulses and/or improve excitation accuracy compared with conventional methods using 3D RF pulses and linear gradients.

METHODS

In source-free regions, magnetostatic fields are governed by the Laplace equation (19):

$$\frac{\partial^2 B_z}{\partial x^2} + \frac{\partial^2 B_z}{\partial y^2} + \frac{\partial^2 B_z}{\partial z^2} = 0, \quad [1]$$

where B_z is the z component of the magnetic field. Mathematically, gradient fields (or gradients) are solutions of the Laplace equation in the form of spherical harmonics. The first-order solutions are linear gradients. The second-order solutions/gradients are usually given in the following forms:

$$z^2 - (x^2 + y^2)/2, x^2 - y^2, xy, yz, \text{ and } xz, \quad [2]$$

which can be available either from specially designed second-order gradient coils (17,18) or more often from second-order shim coils on commercial MRI scanners (20). The Laplace equation limits the choice of a desired nonlinear gradient. For instance, a hypothetical gradient in the form of $x^2 + y^2$ along with a frequency-selective RF

¹Department of Electrical and Computer Engineering, University of Illinois at Urbana-Champaign, Urbana, Illinois, USA

²Beckman Institute for Advanced Science and Technology, University of Illinois at Urbana-Champaign, Urbana, Illinois, USA

³Applied Science Laboratory, GE Healthcare, Milwaukee, Wisconsin, USA

Grant sponsor: NSF; Grant number: NSF-CBET-07-30623; Grant sponsor: NIH; Grant number: NIH-P41-RR023953; Grant sponsor: Beckman graduate fellowship (Chao Ma)

*Correspondence to: Chao Ma, M.S., Beckman Institute for Advanced Science and Technology, 405 N. Mathews Ave, Urbana, Illinois 61801. E-mail: chaoma2@illinois.edu

Received 27 October 2011; revised 22 February 2012; accepted 23 February 2012.

DOI 10.1002/mrm.24259

Published online 5 April 2012 in Wiley Online Library (wileyonlinelibrary.com).

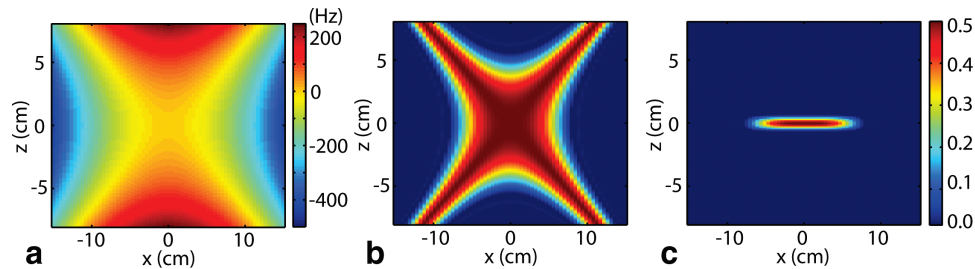


FIG. 1. Reduced FOV excitation using a second-order gradient and a spatial-spectral RF pulse. **a**: The spatial dependence of a 0.9 mT^2 Z2 gradient (in Hz). **b**: The excitation pattern ($|M_{xy}|$) achieved by a 30° frequency-selective RF pulse of 138 Hz bandwidth in the presence of the Z2 gradient in **(a)**. **c**: The excitation pattern achieved by a 30° spatial-spectral RF pulse that selects a 0.7 cm slice with a 138 Hz bandwidth in the presence of the Z2 gradient in **(a)**. Note that the field in **(a)** and the excitation patterns in **(b)** and **(c)** are all cylindrically symmetric around the z axis.

pulse would excite a pencil beam. However, such a field does not satisfy the Laplace equation. In the following, we describe a new method to use second-order gradients and spatial-spectral pulses to excite a circular ROI in a thin slice for reduced FOV imaging.

The basic idea of the proposed method can be illustrated through the following example. Suppose that the target excitation pattern is a circular ROI of radius R in a thin slice of thickness d with a 30° flip angle:

$$|M_{xy}|(x, y, z) = \begin{cases} 0.5, & \text{if } x^2 + y^2 \leq R^2 \text{ and } |z| \leq \frac{d}{2}; \\ 0, & \text{otherwise.} \end{cases} \quad [3]$$

To achieve such an excitation pattern, the conventional approach is to use 3D RF pulses and time-varying linear gradients to cover the 3D excitation k-space, along, for example, spoke trajectories (1,2), which could result in long pulses. In the proposed method, a constant second-order gradient in the form of $z^2 - (x^2 + y^2)/2$ (Z2 gradient) is applied during excitation. Such a Z2 gradient establishes a unique relationship between resonance frequency and spatial location (shown in Fig. 1a). Notably, in the target slice ($|z| \leq \frac{d}{2}$), the resulting excitation pattern of a frequency selective RF pulse is a circular region, and the radius of which (R) can be controlled by the bandwidth of the frequency selective RF pulse (BW):

$$R \approx \sqrt{\frac{BW}{\gamma|G_{Z2}|}}, \quad [4]$$

where G_{Z2} is the magnitude of the Z2 gradient. Equation [4] is valid if the radius of the excitation region is much larger than the slice thickness, i.e., $R \gg d$, which is valid for most reduced FOV imaging applications. However, using the frequency-selective RF pulse and the Z2 gradient alone also results in undesired excitation outside the target slice as shown in Fig. 1b. This problem is overcome in the proposed method using the simultaneous frequency and slice selectivity of a 2D spatial-spectral RF pulse as shown in Fig. 1c. Therefore, by leveraging the unique spatial dependence of the Z2 gradient, a 2D spatial-spectral pulse can achieve 3D spatial selectivity! This dimension reduction means that, with the same pulse length and the same slice selection specification, the proposed method can achieve

larger excitation k-space coverage than the conventional methods using 3D RF pulses and linear gradients, which can lead to shorter pulses and/or better excitation accuracy compared with the conventional method.

We next describe the design of the proposed pulse that consists of a spatial-spectral RF pulse, an oscillating linear gradient in the slice-selection axis (z axis), and a constant Z2 gradient, as illustrated in Fig. 2a. First, we express the waveform of the spatial-spectral pulse as (21,22):

$$b_1(t) = b_{\text{spat}}(t)b_{\text{spec}}(t), \quad [5]$$

where $b_{\text{spat}}(t)$ is a chain of subpulses used for slice selection, and $b_{\text{spec}}(t)$ describes the envelope of the spatial-spectral pulse and defines its spectral response. Note that the above design equation is based on small-tip angle approximation (23), and thus has the same well-known limitations of small-tip angle pulses.

Second, we propose to determine the amplitude of the Z2 gradient G_{Z2} , the oscillating gradient $G_z(t)$, and the RF pulse waveform $b_1(t)$ based on the following considerations/procedures:

1. The oscillating gradient $G_z(t)$ of period T and the slice-selective subpulse of $b_{\text{spat}}(t)$ (e.g., a sinc/Shinnar-Le Roux pulse) are designed using the conventional method to select the desired thin slice ($|z| \leq \frac{d}{2}$).
2. The excitation pattern of the spatial-spectral pulse has a periodic pattern separated by $\frac{1}{T}$ along the frequency axis (shown in Fig. 2b). To avoid exciting the replicates, the amplitude of the Z2 gradient is chosen to satisfy the following relation:

$$f_{\text{max}} \leq f_{\text{rep}} - \frac{BW}{2}, \quad [6]$$

where $f_{\text{max}} = \gamma|G_{Z2}|\frac{L^2}{2}$ is the maximum resonance frequency offset of the imaging object of radius L in the selected slice, $BW = \gamma|G_{Z2}|R^2$ is the bandwidth of the spectral-selective pulse envelope $b_{\text{spec}}(t)$ for exciting a circular ROI of radius R , and $f_{\text{rep}} = \frac{1}{T}$ is the position of the center of the first excitation replicate that has width approximately equal to BW . While satisfying Eq. [6], a stronger second-order gradient allows higher time-bandwidth-product

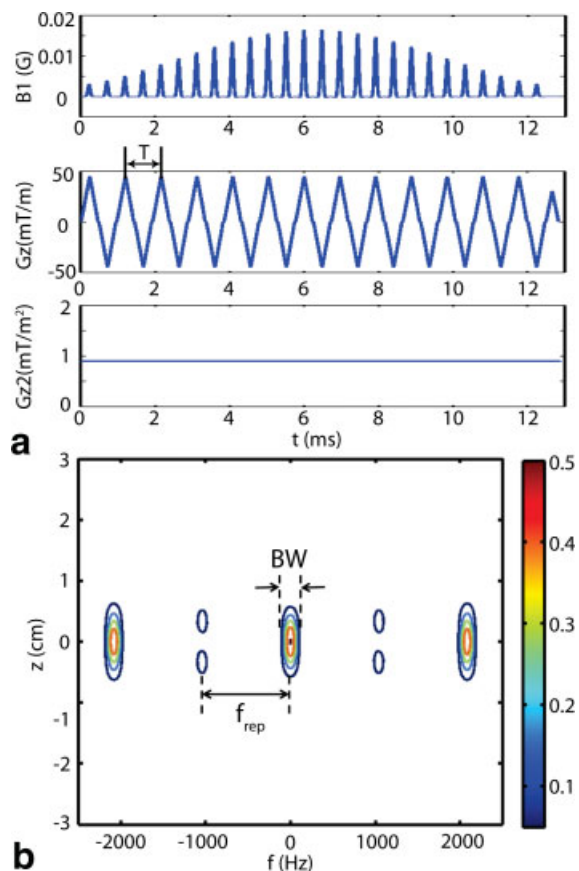


FIG. 2. The proposed pulse consists of a spatial-spectral RF pulse, an oscillating linear gradient, and a constant Z2 gradient as shown in (a), where T is the period of the oscillating linear gradient. In this specific example, the spatial-spectral RF pulse selects a 0.7 cm slice with a 138 Hz bandwidth and a 30° flip angle; the maximum slew rate of the oscillating linear gradient is 200 T/m/s; the magnitude of the Z2 gradient is 0.9 mT/m^2 . The contour plot of the corresponding excitation pattern in the $z-f$ plane is shown in (b), where BW is the bandwidth of the spectral response, and f_{rep} is the position of the first replicate. [Color figure can be viewed in the online issue, which is available at wileyonlinelibrary.com.]

of the spectral-selective pulse envelope $b_{\text{spec}}(t)$, which can improve the in-plane spatial resolution and/or shorten the proposed RF pulse.

3. The spectral-selective pulse envelope $b_{\text{spec}}(t)$ (e.g., a sinc/Shinnar-Le Roux pulse) of length $N \times T$ (resulting in an oscillating gradient of N periods) is designed to define a spectral response of bandwidth BW . The RF pulse $b_1(t)$ is then calculated using Eq. [5].

The discussion so far is focused on exciting a circular ROI in the center of the FOV. Shifting the excitation pattern to an arbitrary position can be done using a combination of first-order and second-order gradients plus frequency offset. Specifically, to excite a circular ROI centered at (x_0, y_0) in a thin slice at z_0 ($|z - z_0| \leq \frac{\Delta}{2}$), we can use the following gradients:

$$\begin{aligned} &G_{Z2}[(z - z_0)^2 - [(x - x_0)^2 + (y - y_0)^2]/2] \\ &= G_{Z2}[z^2 - (x^2 + y^2)/2] \text{ (second-order gradient)} \end{aligned}$$

$$\begin{aligned} &-2G_{Z2}z_0z + G_{Z2}x_0x + G_{Z2}y_0y \text{ (linear gradient)} \\ &+ G_{Z2}[z_0^2 - (x_0^2 + y_0^2)/2] \text{ (frequency offset)}. \end{aligned} \quad [7]$$

The oscillating linear gradient remains the same with added frequency modulations of the subpulse $b_{\text{spat}}(t)$ (24). The design procedure discussed above follows. More generally, it can be shown that an elliptical ROI at an arbitrary location in an oblique slice can be excited with an appropriate combination of frequency offset, three linear and five second-order gradients (12,20).

RESULTS

The proposed method has been validated using Bloch equation simulations and phantom experiments. In the Bloch equation simulation study, we used the proposed method to design an RF pulse (shown in Fig. 2a) that excited a thin disk of 6-cm radius and 0.7-cm thickness in a cylindrical phantom of 15-cm radius with a 30° flip angle (shown in Fig. 3a). The slice-selection gradient waveform was an oscillating triangular waveform of 13 periods, resulting in a 12.8 ms RF pulse. The maximum amplitude and the maximum slew rate in the slice-selection gradient design were chosen to be 50 mT/m and 200 T/m/s, respectively. The slice-selective subpulse was a sinc pulse of a time-bandwidth-product of 3. The magnitude of the Z2 gradient was chosen to be 0.9 mT/m^2 . The spectral-selective pulse envelope was chosen to be a linear-phase Shinnar-Le Roux pulse of 138 Hz bandwidth and with 0.1 ripples in the passband and 0.01 ripples in the stopband. For comparison, a conventional RF pulse using spoke trajectory was designed using a recently proposed method that jointly designed the RF pulse and the spoke locations (25). The time-bandwidth-product of the slice-selective subpulse was also 3. Twenty four spokes were chosen in a 32×32 k-space grid, resulting in a 12.8 ms RF pulse.

The accompanying Z2 gradient is shown in Fig. 1a, and the proposed RF pulse is shown in Fig. 2a. Good slice selectivity was achieved as shown in the excitation pattern of the proposed pulse in the $x-z$ plane (Fig. 1c) and in the $z-f$ plane (Fig. 2b). The in-plane excitation profile is shown in Fig. 3. Compared to the conventional RF pulse using spoke trajectory (Fig. 3b), an excitation pattern of much sharper transition on the edge of the circular ROI and smaller side lobes (especially near the object boundary), was achieved by the proposed pulse (Fig. 3c). The impact in the transition bands can be better seen in the excitation profile plot in Fig. 3d. The through-plane excitation profiles of both methods (results not shown) are very close to each other, as the same slice-selective subpulses were used.

A preliminary experimental study of the proposed method was carried out on a 3.0 T GE whole-body MRI scanner. As the scanner was not equipped with the capability to dynamically adjust the Z2 gradient strength, the proposed pulse was implemented using a static Z2 gradient, which was controlled by changing the shimming current value. To calibrate the Z2 gradient strength, B_0 mapping was performed using a multislice gradient-recall echo sequence. For a given shimming current value, the measured B_0 map was fitted using a field model with up to second-order gradient terms. Although spin-echo imaging would be better for reducing the effects of the static

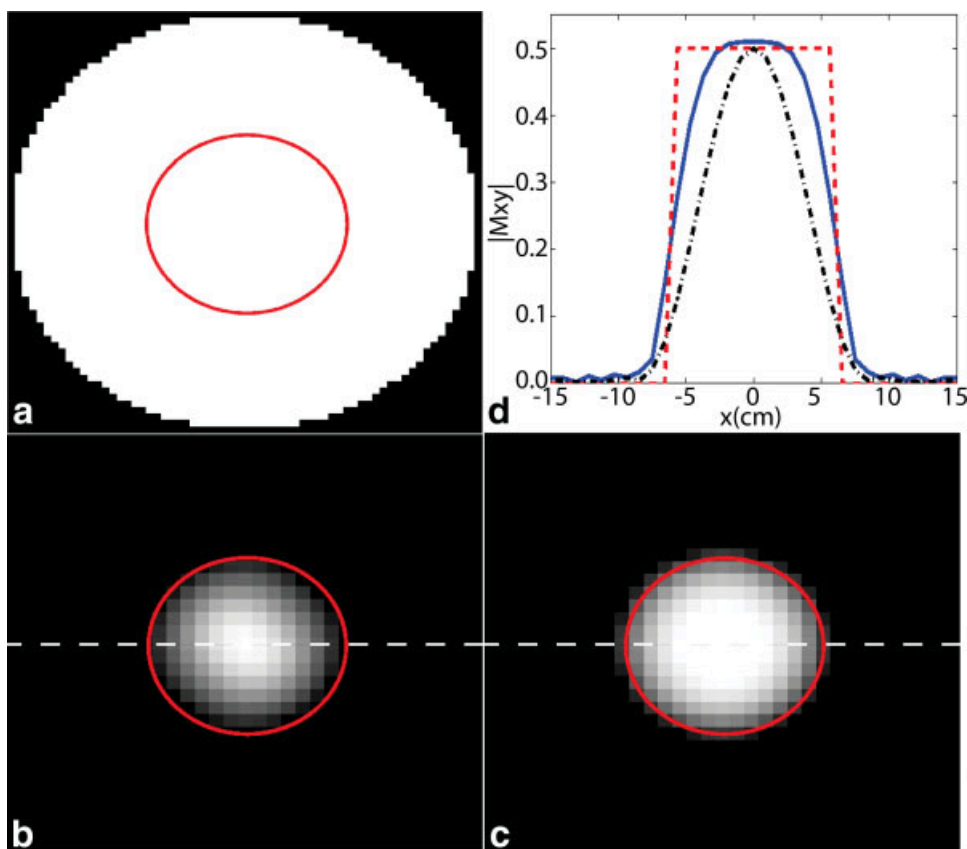


FIG. 3. Excitation patterns in the slice plane achieved by the proposed pulse and a conventional pulse using spoke trajectory. **a:** The desired excitation pattern (indicated by a red circle). **b:** The excitation pattern by the conventional pulse. **c:** The excitation pattern by the proposed RF pulse. **d:** The excitation profiles along the dashed lines (red dashed line: the desired profile; blue solid line: the proposed method; black dash-dotted line: the conventional pulse). [Color figure can be viewed in the online issue, which is available at wileyonlinelibrary.com.]

Z2 gradient during data acquisition, we chose an echo-planar imaging sequence for our experiments because the sequence has a built-in spatial-spectral RF pulse (that was originally designed for fat suppression at 3.0 T). An image-domain postprocessing method (26) with the B_0 map as input was used to reduce the distortions of the echo-planar imaging images caused by the Z2 gradient and the background B_0 inhomogeneity.

The Z2 gradient strength used in the experiments was 0.7 mT/m^2 , whereas the maximum available Z2 gradient of the scanner was about 2.0 mT/m^2 . The parameters of the spatial-spectral pulse used in the experiments were: pulse length 9 ms, main-lobe bandwidth 400 Hz, positions of the first excitation replicates $\pm 800 \text{ Hz}$, and slice thickness

8 mm. The radius of the resulting excitation pattern was 11.5 cm. The position of the first excitation side lobe was at $r = 23.1 \text{ cm}$. The imaging FOV was $48 \text{ cm} \times 48 \text{ cm}$. The experiments were carried out using a phantom consisting of nine tubes containing copper sulfate. Figure 4 shows the experimental results with and without reduced FOV excitation, respectively, which demonstrate that reduced FOV excitation was successfully achieved.

DISCUSSION

Through Bloch equation simulations and phantom experiments on a commercial MRI scanner, we have demonstrated that a second-order gradient can be used along with

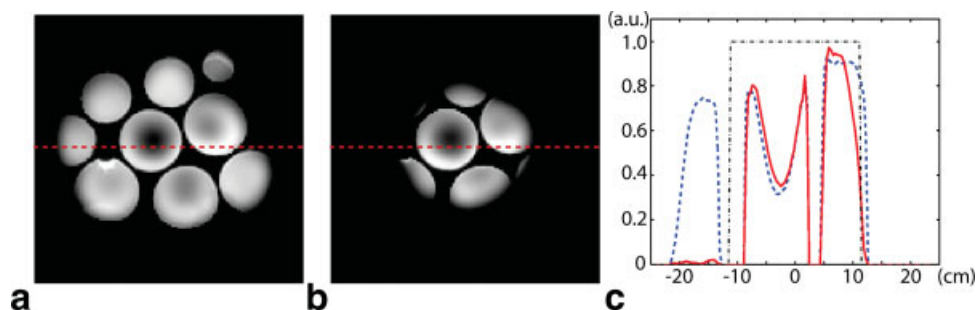


FIG. 4. Experimental results from a phantom consisting of multiple tubes: **(a)** without reduced FOV excitation, **(b)** with reduced FOV excitation using the proposed method, and **(c)** 1D profiles along the dashed lines (black dot-dashed line: the desired ROI; blue dashed line: without reduced FOV excitation; red solid line: with reduced FOV excitation). [Color figure can be viewed in the online issue, which is available at wileyonlinelibrary.com.]

a spatial-spectral RF pulse to excite a circular/elliptical ROI in a thin slice. By taking advantage of the unique multidimensional spatial dependence of second-order gradients, we can effectively reduce the RF pulse length required to achieve multidimensional selectivity. Compared to the PexLoc method described in (14,15), which uses second-order gradients as strong as linear gradients, the proposed method requires only relatively weak second-order gradients. Our preliminary experimental studies demonstrate that reduced FOV excitation can be achieved using second-order gradients readily available on a commercial MRI scanner without requiring specially designed second-order gradient coils and/or amplifiers. However, stronger second-order gradients would make it possible to excite smaller ROIs, increase spatial resolution, and/or shorten the pulse using the proposed method. This is because, for a given pulse length, stronger second-order gradients increase the time-bandwidth-product of the spectral-selective pulse envelope, thus leading to better in-plane spatial selectivity of the proposed pulse.

The unique spatial dependence of second-order gradients is especially suitable for exciting a circular/elliptical ROI. In conventional reduced FOV imaging, 2D RF pulses are designed to excite a rectangular ROI that limits the FOV in the slice and phase-encoding directions (6–8). The FOV in the frequency-encoding direction can be reduced by changing the cutoff frequency of the lowpass filter in the receiver chain. Although the rectangular FOV is desirable for Cartesian sampling trajectories, the circular/elliptical FOV achieved by the proposed method is more suitable for non-Cartesian sampling trajectories, e.g., radial, spiral, and PROPELLER (27) trajectories. Recently, a multicoil technique has been proposed to generate more complex gradients that are beyond second-order gradients through a set of circular individual coils (28,29). When combined with the multicoil technique, the proposed method can excite more flexible ROIs.

Note that the second-order gradient will also introduce phase dispersion among the spins in the excited region. If the second-order gradient is fully controllable, the problem can be easily addressed by adding a rephasing second-order gradient lobe after excitation (as is done in conventional slice selective gradients). If the second-order gradient is static (stays on for the entire imaging period), which is the case for current commercial MRI scanners, it can be treated as an additional term of background B_0 inhomogeneity. Its major effects will be in-plane image distortion, which could be mitigated using large readout gradient and be corrected by B_0 inhomogeneity compensation techniques (26,30) and gradient nonlinearity compensation techniques (31).

CONCLUSIONS

This article presents a new method to design RF pulses for reduced FOV excitation using second-order gradients and spatial-spectral pulses. By leveraging the unique multidimensional spatial dependence of second-order gradients, the proposed method achieves 3D spatial selectivity, i.e., a circular/elliptical ROI in a thin slice, using a 2D spatial-spectral RF pulse. The proposed method is validated using Bloch equation simulation, which shows that the RF pulse dimension reduction achieved by the proposed method can

lead to significantly improved excitation accuracy and/or much shorter pulses compared with conventional 3D RF pulses using linear gradients. Preliminary experimental results further demonstrate that with second-order gradients readily available on a commercial MRI scanner, reduced FOV excitation can be successfully achieved using the proposed method.

REFERENCES

1. Saekho S, Yip CY, Noll DC, Boada FE, Stenger VA. Fast-kz three-dimensional tailored radiofrequency pulse for reduced B_1 inhomogeneity. *Magn Reson Med* 2006;55:719–724.
2. Zelinski AC, Wald LL, Setsompop K, Alagappan V, Gagoski B, Goyal V, Adalsteinsson E. Fast slice-selective radio-frequency excitation pulses for mitigating B_1^+ inhomogeneity in the human brain at 7 tesla. *Magn Reson Med* 2008;59:1355–1364.
3. Stenger VA, Boada FE, Noll DC. Three-dimensional tailored RF pulses for the reduction of susceptibility artifacts in T_2^* -weighted functional. *Magn Reson Med* 2000;44:525–531.
4. Yip CY, Fessler JA, Noll DC. Advanced three-dimensional tailored RF pulse for signal recovery in T_2^* -weighted functional magnetic resonance imaging. *Magn Reson Med* 2006;56:1050–1059.
5. Qin Q, Gore JC, Does MD, Avison MJ, de Graaf RA. 2D Arbitrary shape-selective excitation summed spectroscopy (ASSESS). *Magn Reson Med* 2007;58:19–26.
6. Yang GZ, Gatehouse PD, Keegan J, Mohiaddin RH, Firmin DN. Three dimensional coronary MR angiography using zonal echo-planar imaging. *Magn Reson Med* 1998;39:833–842.
7. Glaser KJ, Felmlee JP, Ehman RL. Rapid MR elastography using selective excitations. *Magn Reson Med* 2006;55:1381–1389.
8. Saritas EU, Cunningham CH, Lee JH, Han ET, Nishimura DG. DWI of the spinal cord with reduced FOV single-shot EPI. *Magn Reson Med* 2008;60:468–473.
9. Katscher U, Bornert P, Leussler C, van den Brink JS. Transmit SENSE. *Magn Reson Med* 2003;49:144–150.
10. Zhu Y. Parallel transmission with an array of transmit coils. *Magn Reson Med* 2004;51:775–784.
11. Lee SY, Cho ZH. Localized volume selection technique using an additional radial gradient coil. *Magn Reson Med* 1989;12:56–63.
12. Oh CH, Hilal SK, Cho ZH, Mun IK. New spatial localization method using pulsed high-order field gradients (SHOT: selection with high-order gradient). *Magn Reson Med* 1991;18:63–70.
13. Wu EX, Johnson G, Hilal SK, Cho ZH. A New 3D localization technique using quadratic field gradients. *Magn Reson Med* 1994;32:242–245.
14. Haas M, Ullmann P, Schneider JT, Ruhm, W, Hennig J, Zaitsev M. Large tip angle parallel excitation using nonlinear non-bijective PatLoc encoding fields. In Proceedings of 18th Annual Meeting of ISMRM, Stockholm, Sweden, 2010. p. 4929.
15. Schneider JT, Hass M, Ohrel S, Lehr H, Ruhm W, Hennig J, Ullman P. Parallel spatially selective excitation using nonlinear non-bijective PatLoc encoding fields: experimental realization and first results. In Proceedings of 19th Annual Meeting of ISMRM, Montreal, Canada, 2011. p. 211.
16. Grissom WA, Sacolick L, Vogel MW. B_1^+ inhomogeneity compensation using 3D parallel excitation is enhanced by simultaneous linear and nonlinear gradient encoding. In Proceedings of 19th Annual Meeting of ISMRM, Montreal, Canada, 2011. p. 2898.
17. Welz AM, Zaitsev M, Jia F, Liu Z, Korvink J, Schmidt H, Lehr H, Post H., Dewney A, Hennig J. Development of a non-shielded PatLoc gradient insert for human head imaging. In Proceedings of 17th Annual Meeting of ISMRM, Honolulu, Hawaii, USA, 2009. p. 3073.
18. Ohrel S, Lehr H, Jaspard F, Ullmann P, Post H. Development of a new high-performance PatLoc gradient system for small-animal imaging. In Proceedings of 18th Annual Meeting of ISMRM, Stockholm, Sweden, 2010. p. 3936.
19. Jin JM. Electromagnetic analysis and design in MRI. Boca Raton, FL: CRC Press; 1998.
20. de Graaf RA, Rothman DL, Nixon TW. Spatial localization with pulsed second-order shims. In Proceedings of 15th Annual Meeting of ISMRM, Berlin, Germany, 2007. p. 1350.

21. Meyer CH, Pauly JM, Macovski A, Nishimura DG. Simultaneous spatial and spectral selective excitation. *Magn Reson Med* 1990;15:287–304.
22. Bernstein MA, King KF, Zhou XJ. *Handbook of MRI pulse sequences*. San Diego: Elsevier Academic Press; 2004.
23. Pauly J, Nishimura D, Macovski A. A k-space analysis of small-tip-angle excitation. *J Magn Reson* 1989;81:43–56.
24. Zur Y. Design of improved spectral-spatial pulses for routine clinical use. *Magn Reson Med* 2000;43:410–420.
25. Ma C, Xu D, King KF, Liang ZP. Joint design of spoke trajectories and RF pulses for parallel excitation. *Magn Reson Med* 2011;65:973–985.
26. Chang H, Fitzpatrick JM. A technique for accurate magnetic resonance imaging in the presence of field inhomogeneities. *IEEE Trans Med Imaging* 1992;11:319–329.
27. Pipe JG. Motion correction with PROPELLER MRI: application to head motion and free-breathing cardiac imaging. *Magn Reson Med* 1999;42:963–969.
28. Juchem C, Nixon TW, McIntyre S, Rothman DL, de Graaf RA. Magnetic field modeling with a set of individual localized coils. *J Magn Reson* 2010;204:281–289.
29. Juchem C, Nixon TW, Brown PB, McIntyre S, Rothman DL, de Graaf RA. Spatial selection through multi-coil magnetic field shaping. In *Proceedings of 19th Annual Meeting of ISMRM, Montreal, Canada, 2011*. p. 385.
30. Sutton BP, Noll DC, Fessler JA. Fast, iterative image reconstruction for MRI in the presence of field inhomogeneities. *IEEE Trans Med Imaging* 2003;22:178–188.
31. Langlois S, Desvignes M, Constans JM, Revenu M. MRI geometric distortion: a simple approach to correcting the effects of non-linear gradient fields. *J Magn Reson Imaging* 1999;9:821–831.